Journal of Intelligent Material Systems and Structures
http://jim.sagepub.com/

Inducing recovery stress of NiTiNb SMA wires using heat of hydration for confining concrete

Eunsoo Choi, Baik-Soon Cho, Joonam Park and Kyoungsoo Park

Journal of Intelligent Material Systems and Structures 2011 22: 1949 originally published online 6 September 2011
DOI: 10.1177/1045389X11420587

The online version of this article can be found at:
http://jim.sagepub.com/content/22/17/1949

Published by:
SAGE
http://www.sagepublications.com

Article

Journal of Intelligent Material Systems and Structures

Journal of Intelligent Material Systems and Structures
22(17) 1949–1957

DOI: 10.1177/1045389X11420587
jim.sagepub.com
SAGE

Inducing recovery stress of NiTiNb SMA wires using heat of hydration for confining concrete

Eunsoo Choi[1], Baik-Soon Cho[*4], Joonam Park[2] and Kyoungsoo Park[3]

Abstract

This study suggests the utilization of heat of hydration of concrete to activate the shape memory effect (SME) of shape memory alloy (SMA) wires embedded in concrete and produce recovery and residual stress on the wires. This method is more convenient than the previous electronic resistance heating. For the purpose, this study prepares NiTiNb SMA wires that show appropriate temperature window for the use of heat of hydration. Axial compressive tests of concrete cylinders confined by the NiTiNb SMA wire jackets are used to prove that the utilization of heat of hydration is valid to generate recovery and residual stress in the SMA wires. The confined cylinders show increased peak strengths and much larger failure strains than those of the plain concrete. The general behavior of the SMA wire-confined specimens in this study is similar to that of specimens heated by electronic heating jacket. Also, this study explains two examples for the utilization of heat of hydration for the SME in reinforced concrete beams and columns.

Keywords

shape memory effect, NiTiNb, concrete, hydration heat, confinement

Introduction

The applications of shape memory alloys (SMAs) for concrete structures in civil engineering are expanding more and more since the alloys show a shape memory effect (SME) or superelastic behavior (SEB). The SME is very useful to provide confinement (Choi et al., 2010a) or introduce prestress on concrete (Czaderski et al., 2006; Maji and Negret, 1998), and the SEB can be used for recovering the residual deformation of concrete structures (Saiidi et al., 2009; Saiidi and Wang, 2006). SMA wires or bars were applied for reinforced concrete beams or columns for the SME or SEB. For SME applications for confining or prestressing concrete, the martensitic SMAs should be heated to A_s, which is the temperature to start austenite, to transform the state of the alloy to austenite and induce recovery stress that acts as confining pressure or prestress. In previous studies, electronic resistance or heating jackets were used to raise the temperature of SMAs (Choi et al., 2008; Li et al., 2007). However, the previous heating methods were not suitable for the embedded SMA wires or bars that should be exposed out of concrete to connect the electronic power cables. The heating jacket was not appropriate for large structure and the effectiveness of the heat transfer was not good for deep embedded SMAs. Both methods used external electronic power, which increases the difficulty of construction. Concrete structures generate heat of hydration during the curing process because an exothermic chemical reaction occurs between cement and water (Wang et al. 2010). The heat of hydration can heat the SMAs embedded in concrete structures and raise the temperature of the SMAs to induce state transformation. For this purpose, the temperature of concrete reaches up to at least A_s. However, controlling the temperature of concrete is almost impossible since it depends on several factors such as the size of a structure, types of cement, water/cement ratio, ambient temperature, and so on. Thus, the temperature window of the SMAs in concrete should be controlled. The temperature windows consist of four temperatures such as M_s, M_f, A_s, and A_f. In heating phase, austenitic state

[1]Department of Civil Engineering, Hongik University, Seoul, Korea
[2]Department of Civil & Environmental Engineering, WonKwang University, Iksan 570-749, Korea
[3]School of Civil & Environmental Engineering, Yonsei University, Seoul, Korea
[4]Department of Civil Engineering, CTRC, Inje University, Kimhae 621-749, Korea

Corresponding author:
Baik-Soon Cho, Associate Professor, Department of Civil Engineering, CTRC, Inje University, Kimhae 621-749, Korea
Email: civcho@inje.ac.kr

starts at A_s and is finished at A_f. In cooling phase reversely, martensitic state starts at M_s and finishes at M_f. The A_s of an SMA should be higher than the highest ambient temperature to be stored in the air and lower than concrete curing temperature to be transformed the state of SMA. Also, the A_f is required to be lower than the concrete curing temperature to complete the state transformation due to hydration heat. The last requirement is that the M_s must be lower than the lowest ambient temperature to maintain the developed recovery stress.

In general, NiTi SMAs are most popular in the civil applications since they show good mechanical properties (DesRoches et al., 2004). However, they show narrow temperature hysteresis between A_s and M_s and, thus, their applications for the SME are restricted for civil structures. NiTiNb SMAs were introduced to overcome the problem and showed relatively wider temperature hysteresis than NiTi SMAs (He et al., 2004; Seigert et al., 2002; Zhang et al., 1991). Also, the temperature hysteresis of the NiTiNb SMAs was widened by introducing prestrain in the alloys (Choi et al., 2010b; Dong et al., 2002). Thus, the A_s at around the temperature of concrete can be archived by applying a specific prestrain on an NiTiNb SMA. The objective of this study is to manufacture an NiTiNb SMA for the utilization of heat of hydration and to prove the confining effect of SMA wire on concrete under the temperature induced by the heat of hydration.

Heat of Hydration of Concrete and NiTiNb SMA Wire

The heat generated by the cement's hydration raises the temperature of the concrete. Dwairi et al. (2010) measured the temperature of prestressed concrete girders and showed that the internal temperature of the concrete reached a maximum of 70°C at 20 h after starting curing of the concrete and was maintained for approximately 4 h. This result corresponded to the analytical results of Wang et al. (2011). The simulation study showed that the maximum temperature of 70°C of a bridge deck of concrete box developed in 20 h. Thus, based on the fact that the maximum temperature of concrete due to the heat of hydration was approximately 70°C, this study intended to prepare an NiTiNb SMA in which A_s and A_f are located at around 70°C. The alloy of Ni_{50}–Ti_{41}–Nb_9 (at. %) was melt by high-frequency vacuum induction; then hot rolling into wires with a diameter of 1.02 mm at 850°C was conducted. The wires were annealed at 850°C for 15 min, and then the wires were deformed into 1.0 mm diameter wires by cold drawing. During the process, it was estimated that 3.88% prestrain was assigned to the wires. The assigned prestrain changed the temperature windows of the alloy measured from differential scanning calorimetry (DSC) as shown in Figure 1. The A_s and A_f of the ingot an hour after accomplishment of melting were measured as −32.44°C and −2.78°C, respectively. However, after assigning the prestrain due to cold drawing, the A_s and A_f of the wires changed to 50°C and 84°C, respectively. The M_s and M_f of the prestrained wires were too low to measure. Thus, the prestrained wires can start to transform to austenitic state under the temperature of 70°C; however, the transformation cannot be completed since the A_f was higher than 70°C.

In the application of SME for civil structures, the temperature windows are of importance since the structures are exposed to the natural environments. In this study, the A_s of the wires should be higher than the highest possible ambient temperature, for example 40°C, in order to store them under ambient temperature. Also, the M_s should be lower than the possible lowest temperature, for example −10°C, to maintain the developed recovery stress of the wires; when the temperature of the wires becomes lower than M_s, the wires lose all recovery stress because of transformation to a martensitic state. The SMA wires prepared in this study satisfied the requirements for M_s and A_s, but were not satisfactory in that the A_f was higher than 70°C.

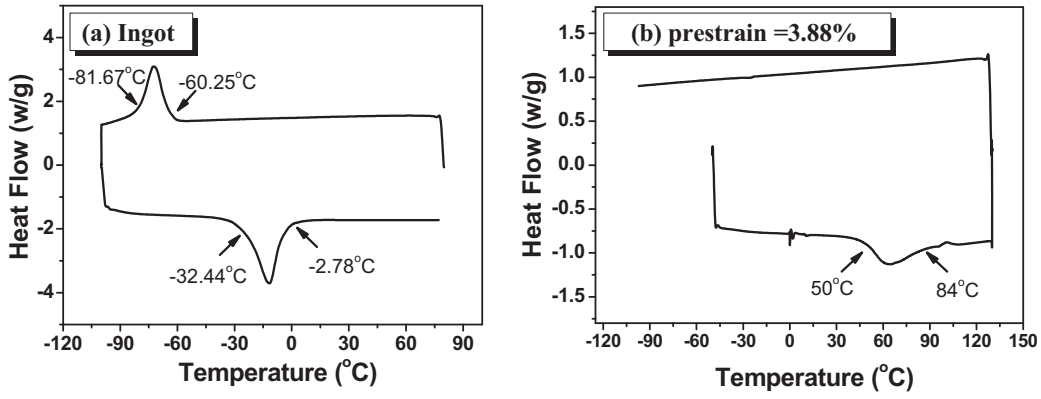

Figure 1. DSC curves for ingot and prestrained wire of the NiTiNb alloy.

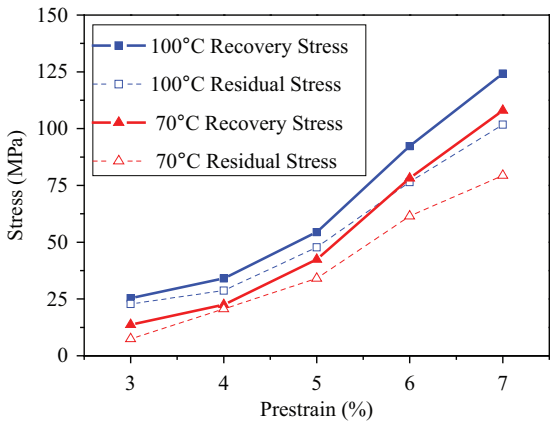

Figure 2. Recovery and residual stress with varying prestrains and temperatures.

The NiTiNb SMA wires with prestrain were heated at 200°C for an hour to recover the residual strain and cooled down to room temperature. Then, the tests for measuring recovery and residual stress with varying prestrains of 3%–7% were conducted. The wires were elongated at room temperature, approximately 15°C, and unloaded to zero stress. Then, the wires were heated to 70°C or 100°C with constraining of the deformation, which generated recovery stress in the wires; wires were then cooled down to room temperature, which reduced the recovery stress; the remaining stress is called residual stress. The temperature 70°C represented that of concrete induced by heat of hydration, and the temperature 100°C, which was higher than the A_f of the wires, was used to transform the wires to austenitic state perfectly. Figure 2 shows the recovery and the residual stress for 70°C and 100°C heating, respectively. The 70°C heating produced smaller recovery stress than the 100°C heating since the 70°C heating partially transformed the SMA wires to austenitic state. Also, the residual stresses due to the 70°C heating were smaller than those for the 100°C heating. When prestrain of 3.88% was assigned, the residual stresses for the 70°C and the 100°C heating were estimated to be 19.03 and 27.98 MPa, respectively, using interpolation. If prestrain of 6% or 7% is assigned to the wires, larger residual stress can be achieved than that by 3.88% prestrain. Larger residual stress is better to provide more external confining pressure. However, the temperature windows of the wires with 6% or 7% prestrain may deviate from the target, and thus the use of 6%–7% prestrain should be considered cautiously.

Specimens and Test Setup

This study chose SMA wire confinement for concrete to investigate the possibility of heat of hydration to induce the SME. Previous studies showed that SMA wires of NiTi or NiTiNb alloy provided external confining pressure on concrete and increased the peak strength and the failure strain of the concrete (Choi et al., 2010a). In the previous studies, a high temperature of 200°C was used to generate full austenitic transformation. This study, following previous studies, used concrete cylinders with dimensions of 150 × 300 mm (Ø × L), and SMA wires as external jackets wrapped around concrete cylinders with a center-to-center pitch of 1.0 mm. Two plain and six SMA wire jacketed cylinders were prepared. Two of six SMA wire jacketed specimens were heated at a temperature of 70°C for an hour in an electronic oven, which simulated the heating by heat of hydration, and then cooled down to room temperature. Two specimens were heated at a temperature of 100°C for an hour and then cooled down to room temperature, at which the SMA wires were perfectly transformed to austenitic state. The last two specimens followed the same procedure as that of the 70°C heated specimens. However, the last specimens were put into a refrigerator for a day to reduce the temperature down to −20°C and were carried in a box of dry ice to maintain the temperature for compressive tests. This simulated the exposure of the specimens to an extremely low-temperature environment. The SMA wire jacketing procedure has been described at length in previous studies. To describe in brief, two anchors were fixed at the top and bottom of a cylinder to fasten the wires, which were wrapped manually. Then, the specimen was placed in an oven and heated to a specific temperature.

The compressive tests were conducted with monotonously increased displacement control of 0.5 mm/min for plain or 1.0 mm/min for confined specimens. The axial and the circumferential deformation were measured using three displacement transducers and a circumferential extensometer, respectively, as shown in Figure 3. The three displacement transducers were located between two sole plates at the top and bottom of the cylinders, and the extensometers were placed at

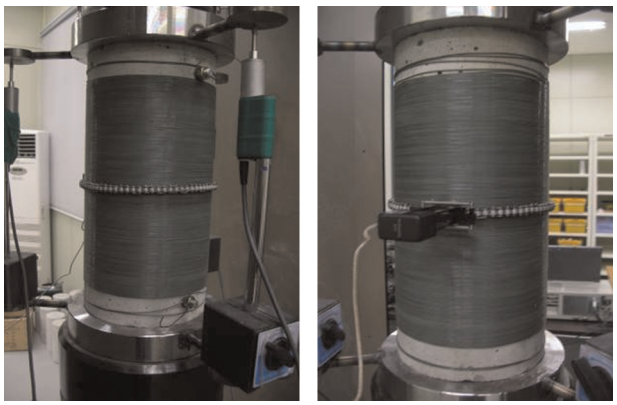

(a) (b)

Figure 3. Test setup for the compressive tests: (a) displacement transducer and (b) extensometer.

Table 1. Specific values of axial compressive tests.

Specimen	f'_{co} or f'_{cc} (MPa)	ε_{co} or ε_{cc} ($\times 10^{-3}$)	f_f (MPa)	ε_f ($\times 10^{-2}$)	k_s	f_e
Plain-1	30.3	2.23	6.96	0.393	—	—
Plain-2	30.3	2.34	3.62	0.592	—	—
70T-1	37.8	5.15	42.7	4.24	1.25	8.6
70T-2	42.6	5.50	38.5	4.43	1.41	9.0
100T-1	43.1	6.05	43.6	4.90	1.42	9.9
100T-2	41.2	4.79	42.4	3.95	1.36	8.0
-20T-1	40.8	4.65	37.8	6.24	1.35	12.7
-20T-2	44.3	5.41	52.9	5.44	1.46	11.1

the middle of the specimens. A preload of 10 kN was applied to confirm contact of the sole plates to the top and bottom surfaces of the concrete cylinders. The measured deformations were used to calculate the axial and the circumferential strain.

Test Results and Discussions

Failure Mode

The 30 mm length at each end of the specimens was not confined by the SMA wires to place the two anchors. Thus, both ends of the confined specimens were started to be crushed after the onset of peak strength, as shown in Figure 4(a). The axial strains of the confined specimens at peak strength were shown up in the third column in Table 1. The corresponding circumferential strains at peak strength were 0.694% and 0.769% for the specimens of 70T and 0.772 and 0.612% for the specimens of 100T, respectively. Then, the inside concrete was crushed, which distorted the round shape of the cylinders (see Figure 4(b)). The middle part of the cylinders bulged greatly with the increasing stroke displacement, and the wires at the middle were fractured and several rounds of wires got lose, as can be seen in Figure 4(c). The circumferential strain for the fracture of the SMA wires was 8.5% although the axial failure strains were different from each other as shown in the fifth column in Table 1. The concrete at the middle, without confinement, was crushed into a saw-like shape as shown in Figure 4(d).

Axial Behavior

The stress–strain curves of the specimens in the axial direction are shown in Figure 5, and the specific values such as peak and failure strength and the corresponding strains appear in Table 1. Also, the table shows the peak strength-increasing factors k_s and the failure strain increasing factor f_e of the confined specimens against the unfenced specimens. The factors are expressed in the equations below:

$$k_s = \frac{f'_{cc}}{f'_{co}} \tag{1}$$

$$f_e = \frac{\varepsilon_{f,\,con}}{\varepsilon_{f,\,un}} \tag{2}$$

where f'_{cc} and f'_{co} are the peak strengths and $\varepsilon_{f,\,con}$ and $\varepsilon_{f,\,un}$ are the failure strains for confined and unconfined concrete, respectively. The SMA wire jackets increased the peak strengths and the failure strains of the

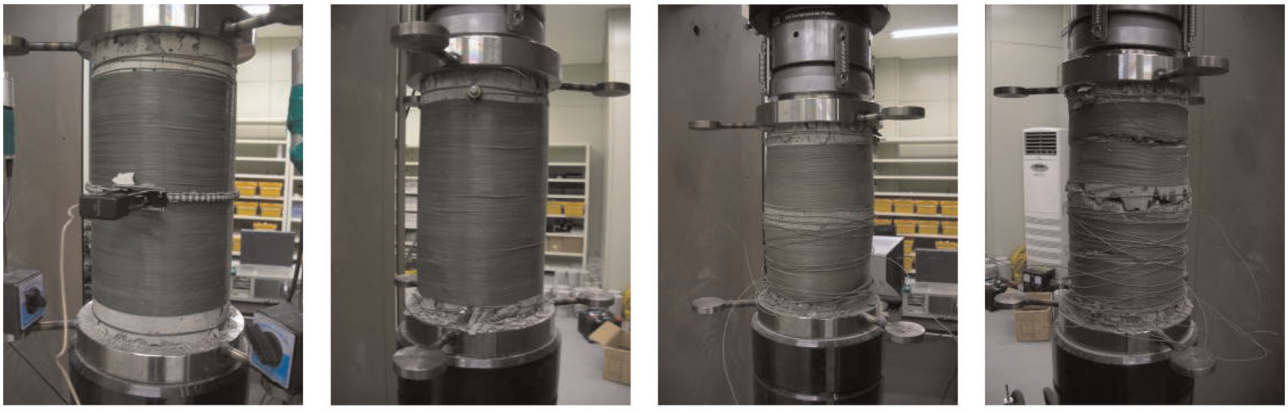

Figure 4. Failure mode of the confined specimens.

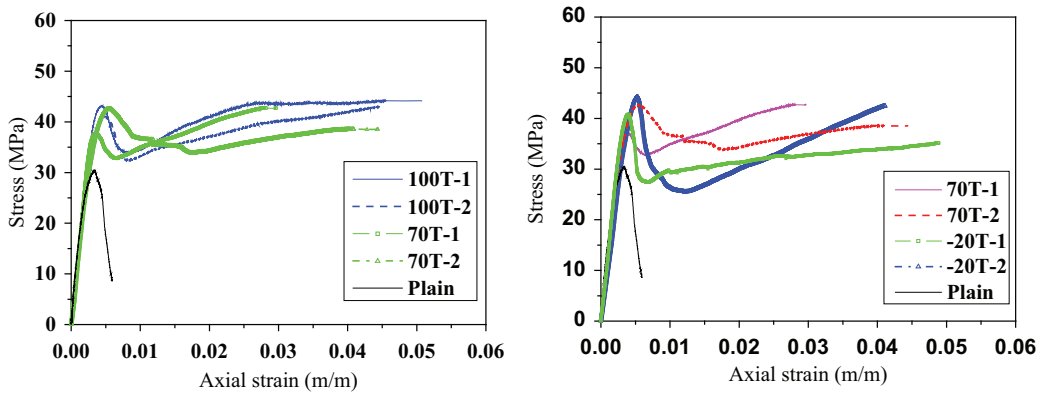

Figure 5. Axial behavior of the confined specimens compared to that of plain concrete cylinder: (a) 100°C versus 70°C and (b) room temperature versus −20°C.

confined specimens as was found in previous studies. The average peak strength increasing factor of the specimens heated to 100°C was 1.39, which was larger by 4.5% than that of the specimens heated to 70°C. However, it seems that both types of the specimens showed a similar peak strength increasing factor considering that a specimen of 70T showed a deviated result. The failure strain increasing factors ranged between 8.0 and 9.9 for both specimens of 70T and 100T.

The SMA wires provided active and passive external confinement in concrete. The passive confinement was provided by the stress developed in the wires due to the lateral bulge of the concrete cylinder. Also provided was active confinement due to the residual stress. If the passive confinement is equal for both types of specimens, only active confinement affects the difference of the peak strength of the concrete. The residual stresses were estimated as 19.03 and 27.98 MPa for specimens heated to 70°C and 100°C, respectively. The active confining pressures were calculated following Equation (3) and estimated as 0.20 and 0.29 MPa, respectively. The effect of active confining on peak strength was so small to neglect, and the above judgment was reasonable. The confining effect will be discussed in detail later.

$$f_l = \frac{2Af_h}{SD} \tag{3}$$

where A = cross-sectional area of SMA wire, f_h = residual stress, S = the spacing pitch, and D = the diameter of the specimen.

The temperature variation of the two confined specimens that were heated to 70°C and, then, cooled down to −20°C is shown in Figure 6. The temperature of the two specimens inside the refrigerator was −21.0°C. The temperatures of the specimens just before starting the tests were 0.26°C and −20.2°C for -20T-1 and -20T-2 specimens, respectively. The time for setting up the specimen of -20T-1 was delayed a little and the temperature rose to 0.26°C. The two specimens showed an average strength increasing factor of 1.41, which was nearly the same value as that of the other types of specimens; this means that SMA wires were not transformed to martensitic state and, thus, maintained a part of the initial residual stress. If the SMA wires are transferred

Figure 6. Temperature variation of -20T- specimens: (a) temperature inside the refrigerator, (b) -20T-1 specimen, and (c) -20T-2 specimen.

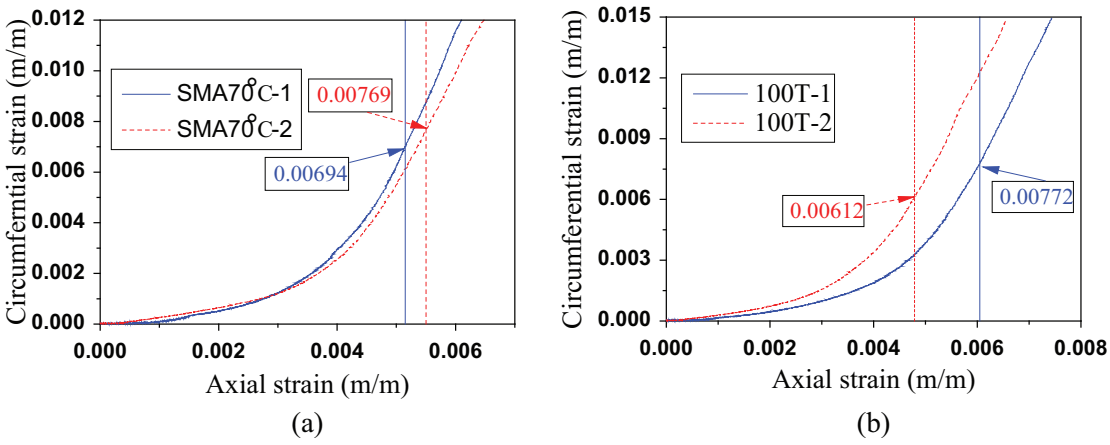

Figure 7. Plot of ratios of circumferential strain to axial strain: (a) SMA 70°C and (b) SMA 100°C.

to martensitic state, the wires lose all residual stress. Under these conditions, the wires neither attach themselves to the concrete surface tightly nor they provide external confinement. Thus, it was found that the M_s of the NiTiNb SMA wires with the 3.88% prestrain was below −20°C. However, the length of the SMA wires shrunk at −20°C due to the thermal effect, which tightened the wires on the concrete surface. If the wires are warmed up to room temperature, the length of the wires is increased; this may affect the test results. The -20T-2 specimen showed a strength-increasing factor of 1.46, the largest among the specimens and a value larger by 8.1% than that of -20T-1 specimen. In general, the residual stress of SMA alloys depends on the temperature, and, thus, the lower temperature provides the lower residual stress. However, the shrinkage of the SMA wires due to low temperature may compensate the relatively low residual stress to provide external confining pressure on concrete. For the room temperature, the residual stress increases and may compensate the expansion of the wires.

Circumferential Behavior

Figure 7 shows the circumferential strains as a function of the axial strain. Following the study of Harries and Kharel (2002), the curves were divided into three parts: (1) initial, (2) transition, and (3) ultimate. The ratio of the circumferential strain to the axial strain was constant in the initial part up to the axial strain of $0.6\varepsilon_{cc}$, where ε_{cc} was the strain at the peak strength in the axial direction. The constant ratio in the initial part represented the Poisson's ratio of the specimen, and the estimated average Poisson's ratios were 0.12 and 0.14 for the 70T and 100T specimens, respectively. These values corresponded to the range of Poisson's ratios of normal concrete, from 0.11 to 0.21 (MacGregor and Wight, 2005). In this range, the passive confining effect was nearly negligible since the lateral bulge was too small. After that, the ratio increased linearly up to $2.0\varepsilon_{cc}$ and became stable again with a constant value. The passive confinement was activated effectively in the transient part due to the large bulges of the specimens. The average peak strains were 0.00533 and 0.00542 for 70T and 100T specimens, respectively. Thus, the values of $0.6\varepsilon_{cc}$ and $2.0\varepsilon_{cc}$ became approximately 0.00322 and 0.0107, respectively. Figure 7 also shows the circumferential strains at the peak strength; the average values were 0.00722 and 0.00691 for 70T and 100T specimens, respectively. These values can be used to calculate the passive confining pressure due to the SMA wire jackets.

Confining Effectiveness

There were about 15 models to assess the confining effectiveness of external or internal confinement of concrete (Moghaddam et al., 2010). Among these, the model proposed by Richart et al. (1928) in the equation below was used in this study.

$$\frac{f'_{cc}}{f'_{co}} = 1 + k_1 \frac{f_l}{f'_{co}} \tag{4}$$

where, f_l is the confining pressure and $k_1$is the confinement effectiveness coefficient; Richart et al. (1928) suggested 4.1 of k_1 for the transverse steel reinforcement. A previous study indicated that the Richart model was well matched to the experimental data of the concrete confined by SMA wire jackets (Choi et al., 2010a). When an external jacket is made of steel or fiber reinforced plastic (FRP), the confining pressure, f_l, at the peak strength is calculated using the yield stress of steel or the fracturing stress of FRP. In this case, the f_h in Equation (3) plays the same role as that of the yield stress of steel or the fracturing stress of FRP. However, for SMA wire jackets, there were active and passive confining pressure, and, thus, the confining pressure, f_l, consisted of the active and the passive pressure and is calculated following the below equation:

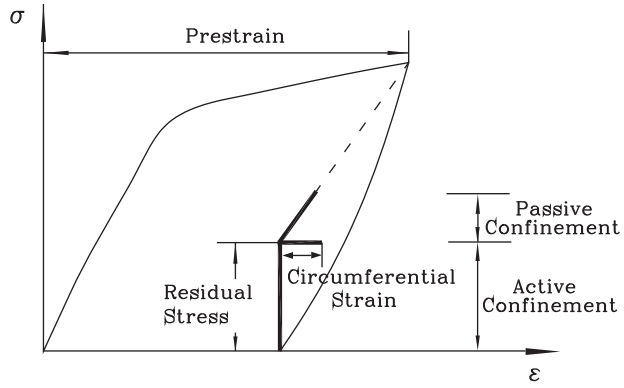

Figure 8. Active and passive stress of SMA wires under residual stress.

$$f_l = f_{l,\,active} + f_{l,\,passive} \quad (5)$$

where $f_{l,\,active}$ and $f_{l,\,passisve}$ represent the active and the passive confining pressure. The active confining pressure is developed due to the residual stress and was estimated in the above section. Determination of the SMA wire behavior under residual stress is necessary to estimate the passive confining pressure. Choi et al. (2010b) showed that the stress–strain curve of SMA wire under residual stress reached the unloading prestrain in an almost linear fashion, as shown in Figure 8. In the figure, the residual stress provided active confinement, and the stress due to additional strain provided passive confinement. The SMA wires were manufactured with 3.88% prestrain, and, thus, this study used values of 4% prestrain for each case to estimate the passive stress on the SMA wires. In Figure 9, the solid lines represent the behavior of the SMA wires under residual stress. The passive stress of the SMA wires was calculated using the slopes of the lines and the circumferential strains. Table 2 shows the estimated active and passive stress of the wires and the active and passive confining pressure for each case. Figure 9 shows the total stresses of the SMA wires including the active and passive stress. The estimated values of k_1 were 7.60 and 8.25 for 70°C and 100°C heating case, respectively. When the data for both cases were used, k_1 was estimated as 7.95, which was larger than the value of 4.33 found in the previous study (Choi et al., 2010a). In general, the mechanical properties of SMA wires vary a great deal due to the components of the SMA alloys and the manufacturing process. Thus, the SMA wire jackets do not produce the same value of k_1 in every case, as steel jackets do (Choi et al., 2010a).

Table 2. Active and passive confining pressure.

Specimen	f_{active} (MPa)	$f_{passive}$ (MPa)	$f_{l,\,active}$ (MPa)	$f_{l,\,passive}$ (MPa)	f_l (MPa)
70T-1	20.6	99.5	0.20	1.05	1.25
70T-2	20.6	110.0	0.20	1.17	1.37
100T-1	28.7	93.7	0.29	0.99	1.28
100T-2	28.7	118.2	0.29	1.25	1.54

f_{active}, $f_{passive}$: stress on the SMA wires.
$f_{l,\,active}$, $f_{l,\,passive}$, f_l: confining pressure due to the stress of the SMA wires.

Discussion and Application

When SMA bars or cables are embedded in concrete, the heating of the SMAs for SME is not easy. In laboratory tests, SMA bars or cables were exposed outside to connect to electric power. The SMA bars or cables were used for civil structures as a kind of reinforcement in longitudinal or transverse directions. Thus, their exposure may produce inconvenience during construction, and the exposed part could be a critical section susceptible to damage due to stress concentration or discontinuity of the concrete surface. The utilization of heat of hydration of concrete can be a very effective heating

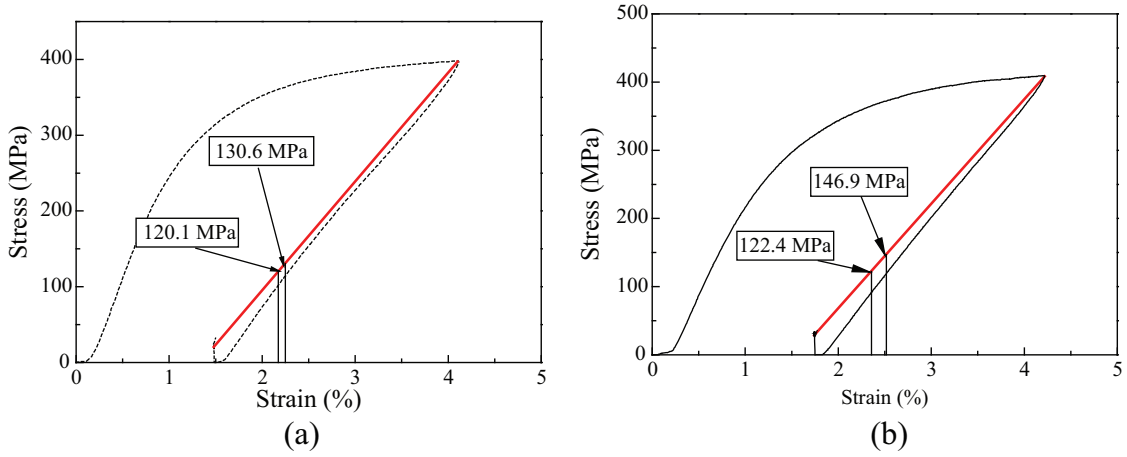

Figure 9. Active and passive stress of the SMA wires: (a) SMA 70°C and (b) SMA 100°C.

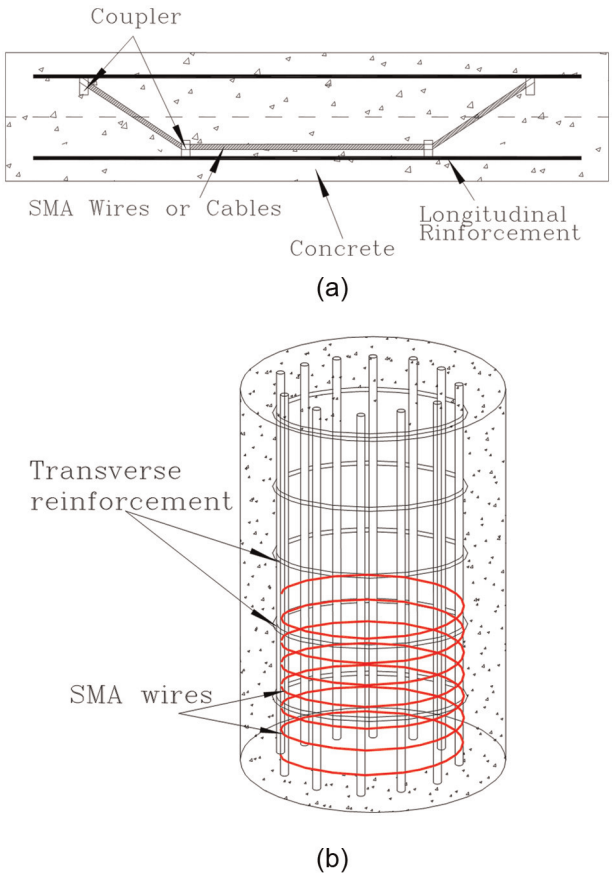

Figure 10. Examples of the use of heat of hydration for the shape memory effect: (a) beam application and (b) column application.

source to induce SME of SMA bars or cables inside concrete. For such a case, the temperature window of the SMAs should be controlled as mentioned above, and the NiTiNb SMA is appropriate for the purpose. The products of precast concrete are generally cured using steam. In such a case, the use of heat of hydration can be more effective since a high enough temperature of concrete can be guaranteed.

Reinforced concrete beams have flexural cracks at the bottom around the midspan and diagonal cracks around one-quarter and three-quarter points. The SMA bars or cables can be used to control such cracks, as shown in Figure 10(a). First, prestrained SMA bars or cables are fixed to the steel reinforcement using couplers, and, then, the heat of hydration of concrete can induce the SME of the SMA bars or cables and develop stress on the bars or cables. The reinforced columns are usually found to fail due to the buckling of the longitudinal reinforcements between transverse reinforcements at the bottom (Choi et al., 2010c). Thus, when prestrained SMA wires are wrapped around a critical section of the longitudinal reinforcement, as shown in Figure 10(b), the SMA wires can be activated by the heat of hydration and provide confining pressure on the longitudinal reinforcement, preventing the buckling of the reinforcement.

Conclusion

This study proposed the utilization of heat of hydration of concrete to induce an SME in SMA bars or wires embedded in concrete; this is considered to be an innovative method compared with previous methods. The NiTiNb SMA alloys are suitable for the purpose since they can show wide temperature hysteresis and their temperature window can be controlled by applying prestrain. This study prepared an NiTiNb SMA alloy to allow for an appropriate temperature window for the use of heat of hydration. Also, this study proved that the concrete temperature due to the heat of hydration activated the SME and provided active confinement in concrete cylinders and that SMA wire jackets increased the peak strength of the confined concrete. However, one point was not perfect, the fact that the A_f of 84°C was higher than the concrete temperature developed by the heat of hydration. The NiTiNb SMA wires were not perfectly performed to an austenite state under 70°C, although the wires started to transform to an austenite state from 50°C. In this study, there was a slight difference between the perfect transformation and the partial transformation of the SMA wires to austenite state since the residual stresses at 70°C and 100°C heating did not show a significant difference. The residual stresses developed in this study were relatively small compared to those seen in the previous study; this was not beneficial to provide large active confinement or prestressing. Thus, it will be necessary, in further studies, to develop NiTiNb SMA alloys that show a proper temperature window for the use of heat of hydration and show large residual stress.

Acknowledgment

This study was supported by the grant from Inje University (2010), and the authors expressed the appreciation for the support.

References

Choi E, Cho S-C, Hu JW, Park T and Chung Y-S (2010b) Recovery and residual stress of SMA wires and applications for concrete structures. *Smart Materials and Structures* 19(094013): 1–10.

Choi E, Chung Y-S, Choi J-H, Kim H-T and Lee H (2010a) The confining effectiveness of NiTiNb and NiTi SMA wire jackets for concrete. *Smart Materials and Structures* 19(035024): 1–8.

Choi E, Chung Y-S, Park J and Cho B-S (2010c) Behavior of reinforced concrete columns confined by new steel-jacketing method. *ACI Structural Journal* 107(6): 654–662.

Choi E, Nam T-H, Cho S-C, Chung Y-S and Park T (2008) The behavior of concrete cylinders confined by shape

memory alloy wires. *Smart Materials and Structures* 17(065032): 1–10.

Czaderski C, Hahnebach B and Motavalli M (2006) RC beam with variable stiffness and strength. *Construction and Building Materials* 20: 824–833.

DesRoches R, McCormic J and Delemont M (2004) Cyclic properties of superelastic shape memory alloy wires and bars. *Journal of Structural Engineering* 130(1): 38–46.

Dong Z, Zhou S and Liu W (2002) A study of NiTiNb shape memory alloy pipe-joint with improved properties. *Materials Science Forum* 394–395: 107–110.

Dwairi HM, Wagner MC, Kowalsky MJ and Zia P (2010) Behavior of instrumented prestressed high performance concrete bridge girders. *Construction and Building Materials* 24: 2294–2311.

Harries KA and Kharel G (2002) Behavior and modeling of concrete subject to variable confining pressure. *ACI Materials Journal* 99(2): 180–189.

He XM, Rong LJ, Yan DS and Li YY (2004) TiNiNb wide hysteresis shape memory alloy with niobium content. *Materials Science & Engineering A* 371: 193–197.

Li L, Li Q and Zhang F (2007) Behavior of smart concrete beams with embedded shape memory alloy bundles. *Journal of Intelligent Material Systems and Structures* 18: 1003–1014.

MacGregor JG and Wight JK (2005) *Reinforced Concrete Mechanics and Design*. 4th Edition. Prentice-Hall, Inc., Singapore.

Maji KA and Negret I (1998) Smart prestressing with shape memory alloy. *Journal of Engineering Mechanics* 124(10): 1121–1128.

Moghaddam H, Samadi M and Pilakoutas K (2010) Compressive behavior of concrete actively confined by metal strips, part B: Analysis. *Materials and Structures* 43: 1383–1396.

Richart FE, Brandtzaeg A and Brown RL (1928) *A Study of the Failure of Concrete under Combined Compressive Stresses*. Urbana Champaign: University of Illinois. 26(12).

Saiidi MS, O'Brien M and Sadrossadat-Zadeh M (2009) Cyclic response of concrete bridge columns using superelastic nitinol and bendable concrete. *ACI Structural Journal* 106(1): 69–77.

Saiidi MS and Wang H (2006) Exploratory study of seismic response of concrete columns with shape memory alloys reinforcement. *ACI Structural Journal* 103(3): 436–443.

Seigert W, Neuking K, Mertmann M and Eggeler G (2002) Influence of Nb content and processing conditions on microstructure and functional properties of NiTiNb shape memory alloys. *Materials Science Forum* 394–395: 361–364.

Wang X-Y, Cho H-K and Lee H-S (2011) Prediction of temperature distribution in concrete incorporation fly ash or slag using a hydration model, Composites Part B: Engineering, 42(1), pp27–40.

Wang X, Lee H, Shin S-W and Golden JS (2010) Simulation of a temperature rise in concrete incorporating silica fume. *Magazine of Concrete Research* 62(9): 637–646.

Zhang CS, Wang YQ, Chai W and Zhao LC (1991) The study of constitutional phases in A Ni47Ti44Nb9 shape memory alloy. *Materials Chemistry and Physics* 28: 43–50.